Journal of Ergonomics
ISSN: 2165-7556

Chang et al., OMICS J Radiology 2013, 2:5
DOI: 10.4172/2167-7964.1000130

Review Article Open Access

Intratumoral Heterogeneity of ^{64}Cu-ATSM Uptake is a Prognostic Indicator in Patients with Cervical Cancer

Albert J Chang[1], Farrokh Dehdashti[2,3], Barry A Siegel[2,3], Michael J Welch[3,4], Julie K Schwarz[1,3,5] and Perry W Grigsby[1,2,3,5]*

[1]*Department of Radiation Oncology, Mallinckrodt Institute of Radiology, USA*
[2]*Division of Nuclear Medicine, Mallinckrodt Institute of Radiology, USA*
[3]*Alvin J. Siteman Cancer Center, USA*
[4]*Division of Radiological Sciences, Mallinckrodt Institute of Radiology, USA*
[5]*Department of Obstetrics and Gynecology, Washington University School of Medicine, St. Louis, Missouri USA*

Abstract

Introduction: Intratumoral heterogeneity determined by FDG-PET is a poor prognostic factor in cervical cancer. Cu-ATSM has been used to evaluate hypoxia in cervical cancer. In this study, FDG and 64Cu-ATSM uptake patterns were compared and the prognostic significance of ^{64}Cu-ATSM heterogeneity was determined.

Methods: 15 patients with cervical cancer who underwent pretreatment ^{64}Cu-ATSM- and FDG-PET/CT were included. The ^{64}Cu-ATSM- and FDG-PET/CT images were co-registered and tumor volumes were autocontoured for each image set in 10% increments of the SUV_{max} ranging from 40% to 80%. The hypoxic fraction defined by ^{64}Cu-ATSM uptake was determined. Concordance between ^{64}Cu-ATSM and FDG uptake was determined by Dice's coefficient. Heterogeneity of ^{64}Cu-ATSM and FDG uptake was calculated as the variance of the 40-80% isothreshold volumes. The association between heterogeneity of ^{64}Cu-ATSM uptake with tumor-specific factors and outcomes was determined.

Results: The hypoxic fraction ranged from 0.773 ± 0.013 to 0.087 ± 0.010 as defined by the 40% to 80% Cu-ATSM isothreshold volumes, respectively. Dice's similarity coefficients for the FDG and 64Cu-ATSM 40 to 80% isothreshold volumes ranged from 0.476 ± 0.012 to 0.112 ± 0.017. Greater ^{64}Cu-ATSM heterogeneity was associated with increased risk of lymph node metastasis at diagnosis (p<0.01), persistent disease after therapy, (p<0.01), and decreased median progression-free survival (11 months vs. not reached, p=0.03).

Conclusion: Significant fractions of cervical tumors are hypoxic. Regions of highest ^{64}Cu-ATSM and FDG uptake were discordant. Elevated ^{64}Cu-ATSM heterogeneity may predict for increased risk of lymph node metastases, decreased responsiveness to treatment, and decreased progression-free survival.

Keywords: FDG-PET; Cervix cancer; IMRT; Brachytherapy

Introduction

Positron Emission Tomography (PET) with F-18 fluorodeoxyglucose (FDG) is indicated for the initial staging of advanced cervical cancer [1] and provides metabolic information about tumors that is not available with anatomic imaging techniques such as CT and MRI. FDG-PET has led to improved disease detection in the pelvic and para-aortic lymph nodes, as well as distant metastases [2]. Several features of FDG-PET images have been shown to correlate with prognosis, including primary tumor FDG uptake, as measured by Standardized Uptake Value (SUV), metabolic tumor volume, and tumor heterogeneity [3].

Hypoxia has been correlated with poor patient survival, therapeutic resistance, and aggressive tumor phenotype. A promising agent for PET imaging of hypoxia is diacetyl-bis (N4-methylthiosemicarbazone) labeled with one of several copper radionuclides (Cu-ATSM). The association of tumor hypoxia and increased Cu-ATSM accumulation has been confirmed in animal studies using oxygen electrode measurements [4]. Clinical studies in patients with lung, rectal, and cervical cancer demonstrated that tumor hypoxia as determined by ^{60}Cu-ATSM accumulation was a negative predictor for treatment response, progression-free survival, and cause-specific survival [5-7].

In a previous study, metabolic heterogeneity on pretreatment FDG-PET/CT was suggested to be predictive of increased risk of lymph node involvement at diagnosis, poor response to therapy, and increased risk of pelvic recurrence in patients with cervical cancer [3]. The derivative of the volume-threshold function (dV/dT) from 40-80% was used as the measure of heterogeneity in that study [3]. A subsequent report suggested that this method was only a surrogate of tumor volume and inaccurate for measuring heterogeneity [8].

Despite this suggestion, tumor heterogeneity has been implicated in disease progression, metastasis, and treatment resistance in many malignancies [9,10]. Hypoxia has been suggested to play a role in tumor heterogeneity leading to dedifferentiation of tumor cells and aggressive growth patterns in neuroblastoma and breast cancer [11]. The role of hypoxia in tumor heterogeneity and cervical cancer outcome is not well-defined. In the current study, we hypothesize that tumor heterogeneity as determined by ^{64}Cu-ATSM uptake predicts for poor clinical outcome. The purpose of this study is to evaluate the relationship between tumor uptake of ^{64}Cu-ATSM and FDG and explore the relationship between ^{64}Cu-ATSM heterogeneity, tumor characteristics, and outcome. A method of measuring heterogeneity

***Corresponding author:** Perry W Grigsby, Washington University School of Medicine, Department of Radiation Oncology–Campus Box 8224, Mallinckrodt Institute of Radiology, St. Louis, MO 63110, USA, Tel: (314) 362-8502; Fax: (314) 747-9557; E-mail: pgrigsby@wustl.edu

Received March 20, 2013; **Accepted** May 15, 2013; **Published** May 21, 2013

Citation: Chang AJ, Dehdashti AJ, Siegel BA, Welch MJ, Schwarz JK, et al. (2013) Intratumoral Heterogeneity of ^{64}Cu-ATSM Uptake is a Prognostic Indicator in Patients with Cervical Cancer. OMICS J Radiology 2: 130 doi:10.4172/2167-7964.1000130

Copyright: © 2013 Chang AJ, et al. This is an open-access article distributed under the terms of the Creative Commons Attribution License, which permits unrestricted use, distribution, and reproduction in any medium, provided the original author and source are credited.

that accounts for tumor volume is proposed and evaluated in this study.

Patients

This is a secondary analysis of data from two separate prospective studies evaluating the role of ^{64}Cu-ATSM-PET/CT in patients diagnosed with cervical cancer. The original studies were approved by the Institutional Review Board (IRB) at Washington University and conducted under IND 62,675 (IND study) on file with the Food and Drug Administration. The subjects participating in these studies gave written informed consent, which included consent to use the study-related data for future secondary analyses. The study population consisted of 15 patients with newly diagnosed, locally-advanced squamous cell carcinoma of the cervix [12]. This analysis included data from 6 of the 10 patients enrolled in a study previously reported by Lewis et al. [13] (the patients for whom images were available at the time of this secondary analysis). The remaining 9 patients were enrolled in an ongoing multicenter trial (ACRIN 6682) [13]. In both protocols, subjects underwent pretreatment whole-body FDG-PET/CT followed by ^{64}Cu-ATSM PET/CT of the pelvis on a separate day. All patients were subsequently treated with concurrent chemotherapy and radiation. FDG-PET/CT images were used to define the extent of the metabolically active disease for radiation treatment planning. The radiation was based on standard Washington University treatment practices for cervical cancer, combining external intensity-modulated radiation therapy (IMRT) and high-dose-rate (HDR) brachytherapy [14]. Chemotherapy consisted of cisplatin (40 mg/m^2 weekly for six cycles) administered concurrently with radiation therapy. The patient characteristics are listed in Table 1.

PET imaging

The details of FDG PET/CT have been previously described [3]. Imaging was performed approximately 60 minutes after administration of an average of 507 MBq (13.7 mCi) (range, 433-555 MBq) of FDG. FDG-PET/CT images were obtained from the base of skull through the proximal thighs, with imaging times of 2-4 minutes per bed position, depending on patient weight. To facilitate clearance of FDG activity from the bladder, a Foley catheter was placed and furosemide (20 mg intravenously) was administered 20 minutes after FDG injection.

					SUV_{max}	
Patient no.	**Age (y)**	**FIGO Stage**	**Pelvic Lymph Node Involvement**	**Para-aortic Lymph Node Involvement**	**^{64}Cu-ATSM**	**FDG**
1	60	IIIB	Yes	Yes	3.3	20
2	65	IIIA	No	No	4.1	8.2
3	79	IVA	No	No	6.6	8.4
4	77	IB2	No	No	6.4	9.6
5	47	IIIB	No	No	3.2	13.4
6	60	IIB	No	No	4.3	9.9
7	70	IIA	Yes	No	5.3	19.2
8	57	IVA	Yes	Yes	6.2	33.1
9	58	IIIB	Yes	Yes	4	17.5
10	48	IIB	No	No	4.6	14.4
11	51	IIIB	No	No	3.0	15.8
12	43	IIIA	No	No	5.0	30.0
13	41	IB2	Yes	No	4.4	4.4
14	40	IIB	Yes	No	6.2	9.4
15	41	IIB	Yes	Yes	6.1	21.9

Table 1: Patient Characteristics.

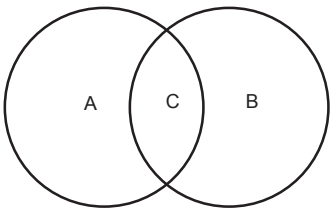

Dice's Similarity Coefficient =2C/(A+B)

A = % 64 Cu-ATSM Isothreshold Volume
B = % FDG Isothreshold Volume
C = Volume of overlap between A and B

Figure 1: Dice's similarity coefficient. A=% FDG isothreshold, B=% ^{64}Cu-ATSM isothreshold, C=overlap volume of A and B.

For the 6 patients on the initial IND study, ^{64}Cu-ATSM was produced as previously described [7]. These patients received a mean of 906 MBq (24.5 mCi) (range, 818-925 MBq) of ^{64}Cu-ATSM and underwent conventional PET imaging on an ECAT HR$^+$ scanner (Siemens-CTI). For the 9 patients on the ACRIN 6682 study, ^{64}Cu-ATSM was produced using a kit formulation and PET/CT was performed as defined in the ACRIN 6682 protocol using a Siemens Biograph 40 scanner [13]. These 9 patients received a mean of 829 MBq (22.4 mCi) (range, 677-914 MBq). Images of the pelvis were acquired for 30 min beginning 30 min post-injection for both studies.

Image analysis

The ^{64}Cu-ATSM images were co-registered to the FDG-PET/CT images using MIMVista 5 software (MIMVista Corp., Cleveland, OH) based on soft tissue and bony pelvic anatomy. Metabolic tumor volumes were autocontoured in 10% increments ranging from 40-80% threshold values of the tumor SUV_{max} on both the ^{64}Cu-ATSM and FDG image sets. Previous work demonstrated that the minimal threshold that represents the actual tumor volume for cervical cancer was 40% [15,16]; therefore, all values <40% were eliminated from the analysis (values <40% represent normal tissue background activity and not tumor). In addition, all values >80% were eliminated because the volumes were small and the partial volume effect was pronounced [17]. Typically, these volumes were <5 cm^3. Contours were reviewed by a physician to ensure that any activity contributed by the bladder and bowel were not included in the region of interest.

To examine the relationship between intratumoral distribution of ^{64}Cu-ATSM and FDG, Dice's similarity coefficient was calculated as illustrated in Figure 1. The fraction of the ^{64}Cu-ATSM 40%, 50%, 60%, 70%, and 80% isothreshold volumes within the 40% FDG isothreshold volume was also calculated for each patient (Figure 1).

Heterogeneity evaluation

To determine FDG and ^{64}Cu-ATSM tumor heterogeneity, the 40%, 50%, 60%, 70%, and 80% isothreshold volumes were determined on each scan. FDG and ^{64}Cu-ATSM heterogeneity was defined as the variance of the 40-80% isothreshold volumes (as demonstrated by the numerator of the equation shown below). The variance for each tumor was normalized to total tumor volume as defined by the 40% isothreshold volume on FDG-PET to account for the role of volume in tumor heterogeneity.

Tumors with large variances in the 40-80% isothreshold volumes

were noted to be more heterogeneous than tumors with low variances in isothreshold volumes.

$$Heterogeneity = \left[\frac{\sum_{i=40\%}^{80\%} (V_i - \overline{V}_i)^2}{(n-1)} \over TotalTumorVolume \right]$$

n=≠ Isothreshhold Intervals

V_i=Volume at each isothreshold interval

V_i=average of isothreshhold volumes

Outcome evaluation

Initial staging, tumor size, and lymph node involvement was determined by clinical examination and by diagnostic FDG-PET/CT. After completion of therapy, patients underwent follow-up physical examinations approximately every 2 months for the first 6 months, every 3 months for the next 2 years, and then every 6 months. FDG-PET/CT was repeated approximately 3 months after completion of treatment and then yearly or when warranted by clinical examination or symptoms. Disease status, including persistent disease 3 months after completion of chemoradiation therapy, pelvic recurrences and distant metastatic disease, were recorded.

Statistical analysis

Regression analysis was used to correlate ^{64}Cu-ATSM heterogeneity with tumor volume. Mann-Whitney non-parametric analysis was used to evaluate the correlation between SUV_{max} for FDG and ^{64}Cu-ATSM and risk of lymph node metastasis at diagnosis, treatment response, and risk of pelvic recurrence. Logistic modeling was used to determine an appropriate cutoff value for ^{64}Cu-ATSM heterogeneity as a predictor of persistent disease as determined by the 3-month post-treatment FDG-PET/CT, as previously described [18]. Chi-square contingency table testing was used to evaluate the correlation between ATSM heterogeneity and FIGO stage, lymph node involvement at diagnosis, and metabolic response on post treatment FDG-PET/CT. Analysis of Progression-Free Survival (PFS) was performed using the Kaplan-Meier method and a log-rank (Mantel-Cox) test. PFS was measured from the completion of radiation treatment. $p<0.05$ was set as the threshold for significance for all study outcomes. All statistical calculations were performed using Stat View for Windows (Version 5.0.1, SAS Institute, Cary, NC).

Results

Patient characteristics

The median age of the patient cohort was 57 years (range, 40-79 years). The median follow-up time for all patients was 16 months (range 5-63 months). The numbers of women with International Federation of Gynecology and Obstetrics (FIGO) clinical stage IB2, IIA, IIB, IIIA, IIIB, and IVA disease were 2, 1, 4, 2, 4, and 2, respectively. In 7 of the 15 patients, the pelvic nodes were positive on pretreatment FDG PET/CT. Para-aortic lymph node involvement was noted in 4 of the patients with pelvic lymph node involvement. Four patients developed recurrent and/or progressive disease with one of these patients dying from disease. Six patients had persistent FDG uptake on their 3-month post-treatment FDG PET/CT scan. Detailed patient characteristics are listed in Table 1.

Tumor characteristics

The mean SUV_{max} for FDG for all tumors was 14.8 ± 6.7 (range 8.2-30.0) and that for ^{64}Cu-ATSM was 4.8 ± 1.2 (range 3.0-6.5). There was no significant correlation between the SUV_{max} for FDG and that for ^{64}Cu-ATSM (R^2=0.011; p=0.90). The SUV_{max} values for ^{64}Cu-ATSM and FDG uptake of each patient are listed in Table 1. There was no significant correlation between tumor volume and the SUV_{max} for ^{64}Cu-ATSM (R^2=0.019; p=0.63) or for FDG (R^2=0.059; p=0.38) (Figure 2). SUV_{max} for FDG-predicted for persistent disease after chemoradiation treatment (p=0.049) but did not predict for the presence of lymph node metastases at diagnosis or disease recurrence (p>0.05). No association was observed between SUV_{max} for ^{64}Cu-ATSM and lymph node involvement, treatment response as determined by the 3-month follow-up PET/CT and clinical examination, nor disease recurrence (p>0.05) (Figure 2).

The similarity between ^{64}Cu-ATSM and FDG uptake volumes was calculated for each lesion using Dice's coefficient (Table 2). A coefficient of 0.113 ± 0.017 (mean ± standard error mean [SEM]) was observed with metabolic tumor volumes generated using the 80% threshold value on the ATSM and FDG images with minimal overlap of regions with high ^{64}Cu-ATSM and FDG uptake in the primary tumor. A representative example is depicted in (Figures 3a and 3b) with the 70% isothreshold volumes contoured in (Figure 3c).

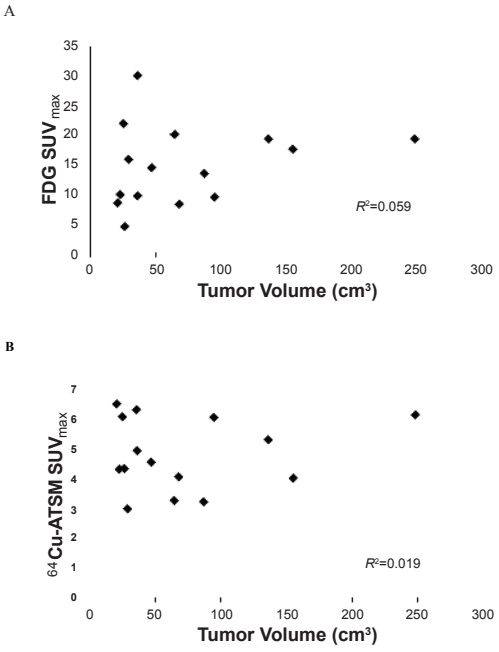

Figure 2: SUV_{max} vs. tumor volume. The relationship between FDG- and ^{64}Cu-ATSM SUV_{max} and tumor volume was plotted in A and B, respectively. There was no correlation between SUV_{max} and tumor volume.

Threshold	Mean ± SEM
40%	0.477 ± 0.012
50%	0.357 ± 0.013
60%	0.238 ± 0.012
70%	0.169 ± 0.016
80%	0.113 ± 0.017

Table 2: Dice Similarity Coefficients for ^{64}Cu-ATSM and FDG Threshold Volumes.

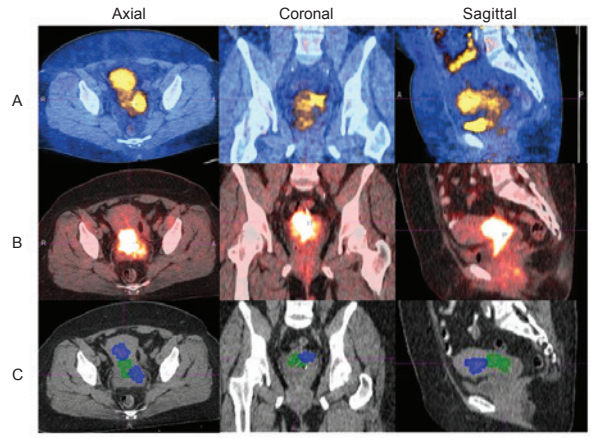

Figure 3: PET/CT images of ^{64}Cu-ATSM in (A) and F-FDG in (B) of a representative patient. The corresponding CT image is demonstrated in (C) with the 70% isothreshold contour from the ^{64}Cu-ATSM images in blue and the 70% isothreshold contour from the FDG images in green. A spatial mismatch is seen between the regions of ^{64}Cu-ATSM and FDG uptake.

Threshold	Mean ± SEM
40%	0.773 ± 0.013
50%	0.536 ± 0.023
60%	0.357 ± 0.024
70%	0.202 ± 0.018
80%	0.087 ± 0.010

Table 3: Fraction of 64Cu-ATSM Threshold Volume Within the FDG Defined Tumor Volume.

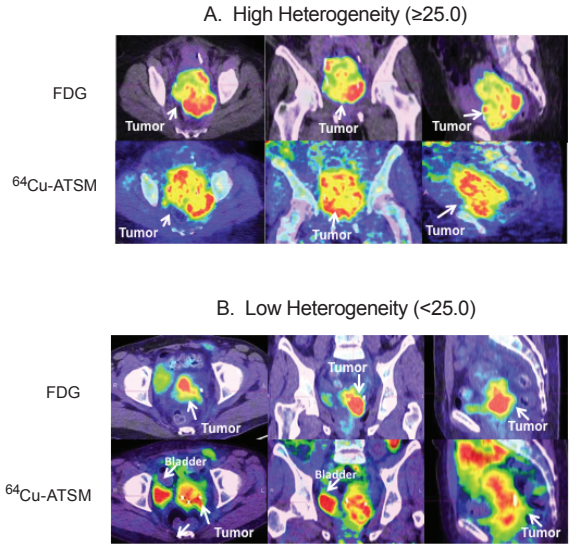

Figure 4: Representative images from two different patients whose tumors have high heterogeneity (*A*) and low heterogeneity (*B*), respectively.

When the thresholding was decreased to 40% for both image sets, the Dice's similarity coefficient was 0.477 ± 0.012 suggesting areas with moderate uptake have a higher degree of overlap. The hypoxic fraction within the primary lesion was also evaluated by analyzing the volume of uptake as defined by the 40%, 50%, 60%, 70%, and 80% isothreshold volumes within the 40% FDG isothreshold volume (Table 3). Areas of significantly greater hypoxia as defined by the 80% and 70% ^{64}Cu-ATSM isothreshold volume accounted for 8.7 ± 1% and 20.2 ± 1.8% of the tumor volume, respectively. Regions of moderate hypoxia as defined by the 60% and 50% isothreshold volume accounted for 35.7 ± 2.4% and 53.6 ± 2.3% of the tumor volume.

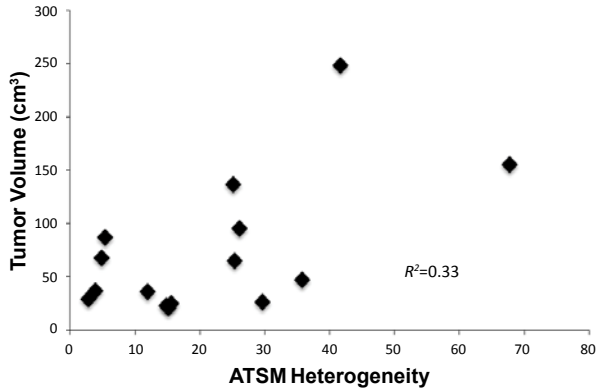

Figure 5: Relationship between tumor volume and ^{64}Cu-ATSM heterogeneity. Each point represents the heterogeneity value plotted against volume for each tumor. No significant correlation between ^{64}Cu-ATSM heterogeneity and tumor volume was observed.

No. of Patients	Heterogeneity <25.0	Heterogeneity ≥ 25.0	p-value
FIGO Stage			
I	0	1	0.73
II	4	3	
III	3	2	
IV	1	1	
Pretreatment lymph node status			
Node positive	1	6	<0.01
Node negative	7	1	
Posttreatment FDG-PET response			
Persistent uptake	0	5	<0.01
No uptake	8	2	

Table 4: ^{64}Cu-ATSM Heterogeneity and Patient Characteristics.

Analysis of intratumoral FDG and ^{64}Cu-ATSM uptake heterogeneity was performed. Figure 4 demonstrates examples of patients with high and low FDG and ^{64}Cu-ATSM heterogeneity. The median heterogeneity of ^{64}Cu-ATSM and FDG uptake was 15.6 (range, 2.8-41.6) and 11.1 (range, 2.6-42.2), respectively. Tumor size did not correlate with ^{64}Cu-ATSM heterogeneity (R^2=0.33, p=0.16) (Figure 5). No relationship was seen between SUV_{max} and heterogeneity for ^{64}Cu-ATSM images. Logistic analysis was used to separate ^{64}Cu-ATSM heterogeneity into high heterogeneity (≥ 25.0) and low heterogeneity (<25.0) groups. The association between ^{64}Cu-ATSM heterogeneity and patient characteristics is summarized in Table 4. High ^{64}Cu-ATSM heterogeneity was not correlated with tumor grade (p=0.80) or FIGO clinical stage (p=0.73). Greater ^{64}Cu-ATSM heterogeneity was associated with the presence of lymph node involvement at diagnosis (p<0.01) and the presence of residual disease as determined by persistent FDG uptake on the posttreatment FDG-PET/CT scan (p<0.01) (Figure 5). In addition, elevated ^{64}Cu-ATSM heterogeneity was associated with poorer PFS. The median progression free survival was 11 months for patients with ^{64}Cu-ATSM heterogeneity ≥ 25.0 and not reached for patients <25.0 (p=0.03, Figure 6).

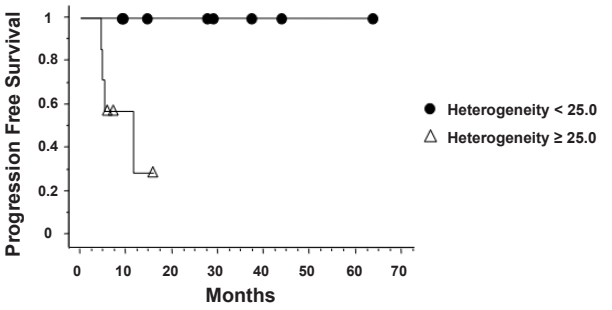

Figure 6: Kaplan-Meier progression-free survival curves for the entire cohort, grouped according to ^{64}Cu-ATSM heterogeneity. Women with cervical tumors having heterogeneity ≥ 25.0 were at significantly increased risk of disease progression. Censor times for heterogeneity <25.0 and ≥ 25.0 are depicted by solid circles and open triangles, respectively.

Discussion

We have evaluated the relationship between FDG and ^{64}Cu-ATSM uptake within primary cervical tumors and the prognostic significance of ^{64}Cu-ATSM heterogeneity. Large fractions of cervical tumors are hypoxic, with regions of greatest hypoxia exhibiting low glucose metabolism as suggested by the inverse relationship between intratumoral ^{64}Cu-ATSM and FDG uptake. To our knowledge, this is the first imaging study to evaluate the relationship between hypoxia and tumor heterogeneity. In a previous report, we found that elevated tumor heterogeneity as determined by FDG uptake was a poor prognostic factor [3]. In the current study, ^{64}Cu-ATSM heterogeneity predicted for increased risk of lymph node involvement at diagnosis, decreased treatment response to chemoradiation, and poorer PFS independent of clinical stage and tumor uptake, as measure by SUV_{max}. These findings demonstrate that tumor heterogeneity, as defined by the variance in ^{64}Cu-ATSM uptake, is a poor prognostic factor.

Several methods have been proposed to evaluate intratumoral hypoxia. The use of Eppendorf oxygen-sensitive electrodes to measure oxygenation status is invasive and provides information limited to the region directly surrounding the probe [19]. Pimonidazole staining requires a biopsy specimen and also provides information limited to the area of biopsy rather than a global picture of intratumoral hypoxia [20]. PET with ^{18}F-fluoromisonidazole (FMISO) has been well characterized as an imaging agent for assessment of hypoxia. However, the relatively low FMISO accumulation within a tumor coupled with delayed clearance from normoxic background tissues results in a low tumor-to-background ratio (<2:1) [21]. Imaging with ^{64}Cu-ATSM results in rapid delineation of tumor hypoxia (in less than 1 h) with high tumor-to-background tissue ratios (tumor-to-blood ratios >>2) [22]. When compared to FMISO, ^{64}Cu-ATSM has increased selectivity for tissues with low oxygen tension [23]. As demonstrated in this study, PET imaging with ^{64}Cu-ATSM is a non-invasive method that provides images detailing the relative severity of hypoxia within different regions of the tumor.

^{64}Cu-ATSM and FDG volumes were autocontoured using multiple isothresholds of the SUV_{max} to compare the spatial distribution of the radiotracers. In a study by Lohith et al. [24,25], regions of interest were manually drawn to evaluate the differences in ^{64}Cu-ATSM and FDG uptake within the tumor [24]. Because generation of the contours was automated in the current study, this method can be easily reproduced in other studies to compare the intratumoral distribution of various tracers and reduces potential observer bias.

Spatial mismatching of tumor ^{64}Cu-ATSM and FDG uptake has been reported in rodent models of gliosarcoma, melanoma and liver, colon, and lung tumors [22,25-27] and in squamous cell lung cancer in humans [24]. Because of the disorganized growth of the tumor vasculature, regional differences in blood perfusion and oxygenation are observed within a tumor [28]. Because FDG uptake may be dependent on blood perfusion, regions of elevated FDG uptake may represent areas that are well vascularized, perfused, and oxygenated [29,30]. In contrast to FDG, ^{64}Cu-ATSM may not be limited by vascular perfusion and can diffuse to greater distances to poorly vascularized and hypoxic regions. This phenomenon has been suggested by an inverse correlation between blood perfusion and ^{62}Cu-ATSM uptake [31]. The differences on the dependence on blood perfusion in tracer uptake may explain the spatial mismatch between FDG and ^{64}Cu-ATSM.

In a previous study, we reported that elevated ^{60}Cu-ATSM uptake predicted for poor prognosis in patients in cervical cancer [32]. Areas of elevated Cu-ATSM and low FDG uptake have been associated with hypovascular regions rich in $CD133^{+}$ cancer stem cells [26,27]. Cancer stem cells are involved in tumor growth, maintenance, and metastases and have been found to be more resistant to radiotherapy and chemotherapy [33]. Cancer stem cells regulate tumor angiogenesis by production of Vascular Endothelial Growth Factor (VEGF) [34,35]. These phenomena may explain the increased risk of lymph node involvement and worse outcomes in patients with greater ^{64}Cu-ATSM heterogeneity in the current study.

A relationship between tumor volume and heterogeneity has been suggested. A previous measure of tumor heterogeneity with FDG-PET was reported using the derivative (dV/dT) of the volume-threshold function from 40% to 80% [3]. This method of measuring tumor heterogeneity was suggested to be inaccurate and only a surrogate for tumor volume [8]. A difficulty exists in separating tumor volume from tumor heterogeneity as, inherently, large volume tumors have a greater potential to become heterogeneous when compared to small tumors. Also, the possibility exists that tumors with greater heterogeneity may grow larger. Hypoxia has been suggested to play a role in tumor heterogeneity [9,20,36]. Under hypoxic conditions, tumors develop more aggressive phenotypes with low apoptotic potential, which can lead to larger tumors [37-39]. Similar to tumor heterogeneity, tumor volume has been associated with clinical stage, with larger tumors presenting at an advanced stage.

To further clarify the relationship between tumor heterogeneity and tumor volume and to evaluate the role of tumor heterogeneity in predicting patient outcome, a novel method of evaluating heterogeneity was proposed in the current study by calculating the variance of the 40-80% isothreshold volumes within the tumor. To account for tumor volume, this variance was normalized to tumor volume. With the proposed measure of heterogeneity, heterogeneous tumors had a speckled pattern of uptake in comparison to tumors with low heterogeneity. We found an association between greater ^{64}Cu-ATSM heterogeneity and the presence of lymph node metastases at diagnosis. Furthermore greater ^{64}Cu-ATSM heterogeneity was associated with shorter PFS independent of FIGO stage. Because of the limited number of patients and follow-up interval, further studies will be needed to validate this measure.

Conclusion

^{64}Cu-ATSM-PET and FDG-PET provide complementary information about the biology of the tumor. The differential uptake

of ^{64}Cu-ATSM and FDG within tumors of the uterine cervix demonstrates that areas of hypoxia have low glucose metabolism and areas of high metabolic activity are better oxygenated. PET imaging with ^{64}Cu-ATSM provides a comprehensive picture of the diversity of hypoxia within a cervical tumor. A novel measure of heterogeneity was defined by calculating the variance of ^{64}Cu-ATSM uptake normalized to tumor volume. With this measure, the degree of ^{64}Cu-ATSM intratumoral heterogeneity predicted for lymph node involvement and decreased PFS. This measure of heterogeneity will be validated in future studies.

Acknowledgements

This work was supported by R01 CA136931-03, DOE grant DE-FG02-87ER60512 and the ACRIN NCI grant U01 CA079778.

References

1. NCCN clinical practice guidelines in oncology: Cervical Cancer. Fort Washington, P.N.C.C.N., 2011. (Accessed 4/13/2011 at.
2. Grigsby PW, Siegel BA, Dehdashti F (2001) Lymph node staging by positron emission tomography in patients with carcinoma of the cervix. J Clin Oncol 19: 3745-3749.
3. Kidd EA, Grigsby PW (2008) Intratumoral metabolic heterogeneity of cervical cancer. Clin Cancer Res 14: 5236-5241.
4. Lewis JS, Sharp TL, Laforest R, Fujibayashi Y, Welch MJ (2001) Tumor uptake of copper-diacetyl-bis(N(4)-methylthiosemicarbazone): effect of changes in tissue oxygenation. J Nucl Med 42: 655-661.
5. Dehdashti F, Grigsby PW, Lewis JS, Laforest R, Siegel BA, et al. (2008) Assessing tumor hypoxia in cervical cancer by PET with 60Cu-labeled diacetyl-bis(N4-methylthiosemicarbazone). J Nucl Med 49: 201-205.
6. Dietz DW, Dehdashti F, Grigsby PW, Malyapa RS, Myerson RJ, Picus J et al. Tumor hypoxia detected by positron emission tomography with 60Cu-ATSM as a predictor of response and survival in patients undergoing Neoadjuvant chemoradiotherapy for rectal carcinoma: a pilot study. Dis Colon Rectum. 2008;51(11):1641-8.
7. Dehdashti F, Grigsby PW, Mintun MA, Lewis JS, Siegel BA, et al. (2003) Assessing tumor hypoxia in cervical cancer by positron emission tomography with 60Cu-ATSM: relationship to therapeutic response-a preliminary report. Int J Radiat Oncol Biol Phys 55: 1233-1238.
8. Brooks FJ, Grigsby PW (2011) Current measures of metabolic heterogeneity within cervical cancer do not predict disease outcome. Radiat Oncol 6: 69.
9. Basu S, Kwee TC, Gatenby R, Saboury B, Torigian DA, Alavi A. Evolving role of molecular imaging with PET in detecting and characterizing heterogeneity of cancer tissue at the primary and metastatic sites, a plausible explanation for failed attempts to cure malignant disorders. European journal of nuclear medicine and molecular imaging.38(6):987-91. doi:10.1007/s00259-011-1787-z.
10. Marusyk A, Polyak K (2010) Tumor heterogeneity: causes and consequences. Biochim Biophys Acta 1805: 105-117.
11. Axelson H, Fredlund E, Ovenberger M, Landberg G, Påhlman S (2005) Hypoxia-induced dedifferentiation of tumor cells--a mechanism behind heterogeneity and aggressiveness of solid tumors. Semin Cell Dev Biol 16: 554-563.
12. Axelson H, Fredlund E, Ovenberger M, Landberg G, Påhlman S (2005) Hypoxia-induced dedifferentiation of tumor cells--a mechanism behind heterogeneity and aggressiveness of solid tumors. Semin Cell Dev Biol 16: 554-563.
13. Lewis JS, Laforest R, Dehdashti F, Grigsby PW, Welch MJ, et al. (2008) An imaging comparison of 64Cu-ATSM and 60Cu-ATSM in cancer of the uterine cervix. J Nucl Med 49: 1177-1182.
14. http://www.acrin.org/TabID/500/Default.aspx.
15. Macdonald DM, Lin LL, Biehl K, Mutic S, Nantz R, et al. (2008) Combined intensity-modulated radiation therapy and brachytherapy in the treatment of cervical cancer. Int J Radiat Oncol Biol Phys 71: 618-624.
16. Miller TR, Grigsby PW (2002) Measurement of tumor volume by PET to evaluate prognosis in patients with advanced cervical cancer treated by radiation therapy. Int J Radiat Oncol Biol Phys 53: 353-359.
17. Showalter TN, Miller TR, Huettner P, Rader J, Grigsby PW. 18F-fluorodeoxyglucose-positron emission tomography and pathologic tumor size in early-stage invasive cervical cancer. Int J Gynecol Cancer. 2009;19(8):1412-4. doi:10.1111/IGC.0b013e3181b62e8c 00009577-200911000-00022 [pii].
18. Soret M, Bacharach SL, Buvat I (2007) Partial-volume effect in PET tumor imaging. J Nucl Med 48: 932-945.
19. Schwarz JK, Siegel BA, Dehdashti F, Grigsby PW (2007) Association of posttherapy positron emission tomography with tumor response and survival in cervical carcinoma. JAMA 298: 2289-2295.
20. Mortensen LS, Buus S, Nordsmark M, Bentzen L, Munk OL, Keiding S et al. Identifying hypoxia in human tumors: A correlation study between 18F-FMISO PET and the Eppendorf oxygen-sensitive electrode. Acta Oncol.49(7):934-40. doi:10.3109/0284186X.2010.516274.
21. Ljungkvist AS, Bussink J, Kaanders JH, van der Kogel AJ (2007) Dynamics of tumor hypoxia measured with bioreductive hypoxic cell markers. Radiat Res 167: 127-145.
22. Imam SK (2010) Review of positron emission tomography tracers for imaging of tumor hypoxia. Cancer Biother Radiopharm 25: 365-374.
23. Dence CS, Ponde DE, Welch MJ, Lewis JS (2008) Autoradiographic and small-animal PET comparisons between (18)F-FMISO, (18)F-FDG, (18)F-FLT and the hypoxic selective (64)Cu-ATSM in a rodent model of cancer. Nucl Med Biol 35: 713-720.
24. Bowen S, Bentzen S, Jeraj R. TH-D-304A: Comparison of Cu-ATSM and FMISO Uptake to Variations in Oxygen Tension. Med Phys. 2009;36:2817.
25. Lohith TG, Kudo T, Demura Y, Umeda Y, Kiyono Y, et al. (2009) Pathophysiologic correlation between 62Cu-ATSM and 18F-FDG in lung cancer. J Nucl Med 50: 1948-1953.
26. Obata A, Yoshimoto M, Kasamatsu S, Naiki H, Takamatsu S, et al. (2003) Intra-tumoral distribution of (64)Cu-ATSM: a comparison study with FDG. Nucl Med Biol 30: 529-534.
27. Tanaka T, Furukawa T, Fujieda S, Kasamatsu S, Yonekura Y, et al. (2006) Double-tracer autoradiography with Cu-ATSM/FDG and immunohistochemical interpretation in four different mouse implanted tumor models. Nucl Med Biol 33: 743-750.
28. Yoshii Y, Furukawa T, Kiyono Y, Watanabe R, Waki A, Mori T et al. Copper-64-diacetyl-bis (N4-methylthiosemicarbazone) accumulates in rich regions of CD133+ highly tumorigenic cells in mouse colon carcinoma. Nucl Med Biol.37(4):395-404. doi:S0969-8051(09)00301-1 [pii] 10.1016/j.nucmedbio.2009.12.011.
29. Carmeliet P, Jain RK (2011) Molecular mechanisms and clinical applications of angiogenesis. Nature 473: 298-307.
30. Janssen MH, Aerts HJ, Buijsen J, Lambin P, Lammering G, Ollers MC. Repeated positron emission tomography-computed tomography and perfusion-computed tomography imaging in rectal cancer: fluorodeoxyglucose uptake corresponds with tumor perfusion. Int J Radiat Oncol Biol Phys. doi:S0360-3016(10)03452-8 [pii] 10.1016/j.ijrobp.2010.10.029.
31. Malinen E, Rødal J, Knudtsen IS, Søvik Å, Skogmo HK (2011) Spatiotemporal analysis of tumor uptake patterns in dynamic (18)FDG-PET and dynamic contrast enhanced CT. Acta Oncol 50: 873-882.
32. Fujibayashi Y, Taniuchi H, Yonekura Y, Ohtani H, Konishi J, et al. (1997) Copper-62-ATSM: a new hypoxia imaging agent with high membrane permeability and low redox potential. J Nucl Med 38: 1155-1160.
33. Dehdashti F, Mintun MA, Lewis JS, Bradley J, Govindan R, et al. (2003) In vivo assessment of tumor hypoxia in lung cancer with 60Cu-ATSM. Eur J Nucl Med Mol Imaging 30: 844-850.
34. Eyler CE, Rich JN (2008) Survival of the fittest: cancer stem cells in therapeutic resistance and angiogenesis. J Clin Oncol 26: 2839-2845.
35. Bao S, Wu Q, Sathornsumetee S, Hao Y, Li Z, et al. (2006) Stem cell-like glioma cells promote tumor angiogenesis through vascular endothelial growth factor. Cancer Res 66: 7843-7848.
36. Borovski T, De Sousa E Melo F, Vermeulen L, Medema JP (2011) Cancer stem cell niche: the place to be. Cancer Res 71: 634-639.
37. Borovski T, De Sousa E Melo F, Vermeulen L, Medema JP (2011) Cancer stem cell niche: the place to be. Cancer Res 71: 634-639.

38. Vaupel P (2010) Metabolic microenvironment of tumor cells: a key factor in malignant progression. Exp Oncol 32: 125-127.

39. Gerlee P, Anderson AR (2007) An evolutionary hybrid cellular automaton model of solid tumour growth. J Theor Biol 246: 583-603.